Metabolic flexibility of a prospective bioremediator

Marozava, Sviatlana; Vargas-López, Raquel; Tian, Ye; Merl-Pham, Juliane; Braster, Martin; Meckenstock, Rainer U.; Smidt, Hauke; Röling, Wilfred F.M.; Westerhoff, Hans V.

published in
Environmental Microbiology
2018

DOI (link to publisher)
10.1111/1462-2920.14295

document version
Publisher's PDF, also known as Version of record

environmental microbiology

Environmental Microbiology (2018) **20**(7), 2652–2669 doi:10.1111/1462-2920.14295

Metabolic flexibility of a prospective bioremediator: *Desulfitobacterium hafniense* Y51 challenged in chemostats

Sviatlana Marozava,[1*] Raquel Vargas-López,[2] Ye Tian,[3] Juliane Merl-Pham,[4] Martin Braster,[2] Rainer U. Meckenstock,[1†] Hauke Smidt,[3] Wilfred F.M. Röling[2‡] and Hans V. Westerhoff[2,5,6]

[1]*Institute of Groundwater Ecology, Helmholtz Zentrum München, Ingolstädter Landstraße 1, 85764, Neuherberg, Germany.*

[2]*Molecular Cell Physiology, Faculty of Science, VU University Amsterdam, De Boelelaan 1085, 1081, HV, Amsterdam, The Netherlands.*

[3]*Laboratory of Microbiology, Wageningen University, Wageningen, The Netherlands.*

[4]*Core Facility Proteomics, Helmholtz Zentrum München, Heidemannstraße 1, 80939, München, Germany.*

[5]*Synthetic Systems Biology, SILS, University of Amsterdam, Amsterdam, The Netherlands.*

[6]*Manchester Centre for Integrative Systems Biology, School of Chemical Engineering and Analytical Science, University of Manchester, Manchester, UK.*

Summary

***Desulfitobacterium hafniense* Y51 has been widely used in investigations of perchloroethylene (PCE) biodegradation, but limited information exists on its other physiological capabilities. We investigated how *D. hafniense* Y51 confronts the debilitating limitations of not having enough electron donor (lactate), or electron acceptor (fumarate) during cultivation in chemostats. The residual concentrations of the substrates supplied in excess were much lower than expected. Transcriptomics, proteomics and fluxomics were integrated to investigate how this phenomenon was regulated. Through diverse regulation at both transcriptional and translational levels, strain Y51 turned to fermenting the excess lactate and disproportionating the excess fumarate under fumarate- and lactate-limiting conditions respectively. Genes and proteins related to the utilization of a variety of alternative electron donors and acceptors absent from the medium were induced, apparently involving the Wood–Ljungdahl pathway. Through this metabolic flexibility, *D. hafniense* Y51 may be able to switch between different metabolic capabilities under limiting conditions.**

Introduction

Perchloroethylene (PCE) is a prevalent soil and groundwater contaminant (Bradley and Chapelle, 2010). Utilization of the reductive dechlorination (RD) activity of organohalide respiring bacteria (OHRB) is an attractive option for efficient and cost-effective remediation of PCE-contaminated sites (Smidt and de Vos, 2004; Bradley and Chapelle, 2010). *Desulfitobacterium* spp. are facultative OHRB, able to synthesize the corrinoid cofactor vitamin B_{12} *de novo*, which is required for reductive dehalogenation; they are also able to grow relatively fast, and are easy to maintain in pure culture (Suyama *et al*., 2001; Nonaka *et al*., 2006; Kim *et al*., 2012; Peng *et al*., 2012). A member of *Desulfitobacterium* spp., *D. hafniense* strain Y51 uses only one reductive dehalogenase thereby performing RD of PCE only to *cis*-DCE (1,2-dichloroethylene) (Furukawa *et al*., 2005). Strain Y51 can use several electron donors (e.g., lactate, formate and pyruvate) and electron acceptors (e.g., sulfate, nitrate, fumarate and organohalides) (Furukawa *et al*., 2005; Villemur *et al*., 2006; Peng *et al*., 2012). Its genome encodes genes for the use of dimethyl sulfoxide (DMSO) and a large number of molybdooxidoreductases, as well as for nitrogen fixation (Nonaka *et al*., 2006; Kim *et al*., 2012). The versatile metabolism promised by the above suggests that *D. hafniense* Y51 might be able to survive in a great variety of environments and might be a successful co-culturing member for the obligate OHRB that are incapable of corrinoid synthesis but able to further reduce *cis*-DCE to non-toxic compounds. Kinetic modelling on competition of OHRB in the environment suggests that biostimulation

Received 1 June, 2017; accepted 19 May, 2018. *For correspondence. E-mail s.marozava@gmail.com; Tel: +49(0)89 3187-3205; Fax: +49(0)89 3187-3361

†Present address: University of Duisburg-Essen, Biofilm Center, Universitätsstr. 5, 41451 Essen, Germany.

‡Wilfred F.M. Röling, originally the lead author of this manuscript, unfortunately passed away on the 25th of September 2015.

Table 1. Gibbs energies of various processes, which might take place in lactate- or fumarate-limited chemostats; calculated for chemical standard conditions ($\Delta G'_0$), for chemostat standard conditions at 35°C ($\Delta G'_{chemst35}$), and for environmental standard conditions at 12°C ($\Delta G'_{envst12}$).

Reactions	$\Delta G'_0$, kJ mol^{-1}	$\Delta G'_{chemst35C}$, kJ mol^{-1}	$\Delta G'_{envst12C}$, kJ mol^{-1}
Fumarate reduction by lactate to succinate and acetate (Process 1)			
$C_3H_5O_3^- + H_2O + 2C_4H_2O_4^{2-} \rightarrow C_2H_3O_2^- + 2C_4H_4O_4^{2-} + CO_2$	−180.8	−148.2	−193.4
Fumarate disproportionation into succinate and carbon dioxide (Process 2)			
$7C_4H_2O_4^{2-} + 4H_2O + 2H^+ \rightarrow 6C_4H_4O_4^{2-} + 4CO_2$	−460.9	−387.2	−490.6
Lactate fermentation to ethanol and carbon dioxide (Process 3)			
$C_3H_5O_3^- + H^+ \rightarrow C_2H_5OH + CO_2$	−18.4	−13.3	−21.2
Lactate fermentation to acetate, carbon dioxide and hydrogen (Process 4)			
$C_3H_5O_3^- + H_2O \rightarrow C_2H_3O_2^- + CO_2 + 2H_2$	−8.8	−34.6	−57.8

Calculations of free Gibbs energies are described in section on 'Experimental procedures'.

(addition of fermentable substrates) may speed up the overall process of dehalogenation if PCE-to-*cis*-DCE-reducing bacteria (e.g*., Desulfitobacterium* spp.) can successfully co-exist with *cis*-DCE-to-ethene-reducing bacteria (e.g., *Dehalococcoides mccartyi*) (Becker, 2006). Getting insights into the physiology of *D. hafniense* Y51 should help to predict its fitness for such scenarios and aid the design for bioremediation strategies.

Despite the wealth of studies on dehalogenation capabilities of *D. hafniense* Y51, knowledge on the regulation of its physiology is limited. *D. hafniense* Y51 has been mainly investigated in batch cultures (Suyama *et al*., 2001; Furukawa *et al*., 2005; Peng *et al*., 2012). In such batch cultures, the initial excess of substrates first leads to adaptation, then to exponential growth and then to more linear growth or even stationary phase as the substrate runs out. In the environment, microorganisms are exposed to various limitations, and the dynamics of those limitations tend to be different. An example is the unbalanced concentrations of electron donor and electron acceptor in contaminated sites, where the concentrations of pollutants (e.g., PCE) can greatly exceed concentrations of electron donors required for their reduction. This happens especially in the plume fringes where electron donors are being consumed rapidly (Meckenstock *et al*., 2015).

As mRNAs, proteins and metabolites have dissimilar life times, understanding the causal relations between their concentrations is straightforward only if they are all at steady state. Because we aimed to examine these relations under variations of well-defined limitations, we grew the organism in chemostat (Kovarova-Kovar and Egli, 1998; Hoskisson and Hobbs, 2005; Rossell *et al*., 2006). Although this approach does not mimic the quick, complex and often spurious changes between diverse limitations that may happen in the environment (see above), it does mimic bacterial growth in the environment when substrates are slowly released from the sediments or soil particles (Esteve-Núñez *et al*., 2005) and thus enhances data interpretation.

In the present study, we aimed to examine the regulation of *D.* hafniense strain Y51 physiology under electron donor (lactate) or electron acceptor (fumarate) limitation in chemostats. As utilization of PCE is cumbersome due to its high volatility, we chose fumarate as a model electron acceptor because it resembles PCE structurally and is not involved in nitrogen or sulfur metabolism. The inflow concentrations of lactate in the chemostats were similar to the initial concentrations of lactate in batch and reflect the high concentration of electron donors added during bioaugmentation. Fumarate concentrations were chosen so as to accomplish proper electron donor or electron acceptor limitation.

Assessing the physiology of *D.* hafniense strain Y51 by combined transcriptomic, proteomic, fluxomic and thermodynamic analysis, we found that it adapted its physiology in a variety of ways, as if trying to benefit from substrates that were or might have been supplied.

Results

Virtually complete utilization of the excess substrates under limiting conditions

During cultivation in batch at maximum specific growth rate of 0.075 ± 0.01 h^{-1}, *D. hafniense* Y51 reduced 2 molecules of fumarate to 2 molecules of succinate via coupling oxidation of 1 molecule of lactate to 1 molecule of acetate (Process 1 in Tables 1 and 2).

If *D. hafniense* Y51 were metabolically inflexible, they should follow Process 1 independently of limitations applied. However, in lactate-limited chemostats (fumarate: lactate inflow ratio of 3), the 20 mM of fumarate expected in the efflux was not detected (Table 2). Nor was the expected excess lactate (5 mM) detected in the outflow in fumarate-limited chemostat F1 (fumarate: lactate inflow ratio of 1.5) (Table 2). In order to examine whether the limitations imposed in fumarate-limited chemostat F1 were not strong enough, we further lowered the fumarate to lactate ratio in the influx of chemostat F2 to 1.3 but without effect; all lactate was still completely consumed. When in chemostat F3 fumarate:lactate inflow ratio of 1.1 was applied some of the inflowing lactate (25%) was detected in the outflow, still 7 mM less than expected according to Process

Table 2. Analysis of five chemostat cultures of *D. hafniense* Y51 in steady state, grown under lactate- and fumarate-limiting conditions and in batch culture.

		Conditions in chemostat inflow					Batch	
		Lactate limitation		Fumarate limitation				
		L1	L2	F1	F2	F3	B1	B2
Inflow concentrations	Lactate (mM)	20	20	20	20	30	20	20
	Fumarate (mM)	60	60	30	25	35	25	25
	Yeast extract (CmM)	4.1	4.1	4.1	4.1	4.1	4.1	4.1
Outflow concentrations	Lactate (mM)	0.0 ± 0.2	0.0 ± 0.1	0.0 ± 0.0	0.0 ± 0.0	5.2 ± 0.1	2.3 ± 0.1	2.1 ± 0.2
	Fumarate (mM)	0.1 ± 0.0	0.0 ± 0.0	0.0 ± 0.0	0.0 ± 0.0	0.0 ± 0.0	0.0 ± 0.0	0.0 ± 0.0
	Acetate (mM)	10.9 ± 0.0	12.3 ± 0.3	13.1 ± 0.3	15.1 ± 0.3	21.1 ± 0.3	12.9 ± 0.2	12.9 ± 1.1
	Succinate (mM)	52.1 ± 1.4	51.0 ± 1.3	25.8 ± 0.1	25.2 ± 0.4	27.3 ± 0.4	23.9 ± 0.2	23.4 ± 1.8
	Biomass (CmM)	14.0 ± 0.3	11.1 ± 0.0	13.5 ± 0.0	5.0 ± 0.1	12.0 ± 0.1	ND	ND
Inflow ratio	Fumarate: lactate	3.0	3.0	1.5	1.3	1.1	1.3	1.3
Observed consumption ratio	Fumarate:lactate	3.0	3.0	1.5	1.3	1.4	1.4	1.4
Substrate consumed/product produced ratio	e-donor Lactate:acetate	1.8	1.6	1.5	1.3	1.2	1.4	1.4
	e-acceptor Fumarate:succinate	1.1	1.2	1.2	1.0	1.2	1.0	1.1
Expected in outflow (mM)[a]	Fumarate	20	20	0	0	0	0.0	0.0
Expected in outflow (mM)[a]	Lactate	0	0	5	7.5	13	7.5	7.5
Recovery (%)[b]	Acetate/Lactate	55	62	66	76	85	73	72
	Succinate/Fumarate	87	85	86	101	78	96	94
Total carbon recovery (%)[c]		84	83	85	92	84	ND	ND
Total e-recovery (%)[d]		91	89	86	90	83	ND	ND
Number cells ml^{-1}		ND	ND	ND	ND	ND	$9.8\ 10^7$	$7.3\ 10^7$
Biomass (dry weight mg l^{-1})		345 ± 6.4	273 ± 0.0	332 ± 0.7	124 ± 1.4	296 ± 2.8	ND	ND
Growth yield (mg dry weight substrate (C)mol^{-1})[e]	/mol lactate	17.3	13.7	16.6	6.2	11.9	ND	ND
	/Cmol lactate	5.8	4.6	5.5	2.1	4.0	ND	ND
	/mol fumarate	5.8	4.6	11.1	5.0	8.5	ND	ND
	/Cmol fumarate	1.4	1.1	2.8	1.2	2.1	ND	ND
	/Cmol Lactate + Fumarate	1.2	0.9	1.8	0.8	1.4	ND	ND
	%Cmol biomass/(Cmol lactate +fumarate)	4.7	3.7	7.5	3.2	5.6	ND	ND

ND, Not determined.
Outflow concentrations and biomass were measured in duplicate.
[a]Expected values were calculated based on Process 1 (Table 1) (taking into account only inflow concentrations), incorporation into biomass was not considered.
[b]Carbon recovery of lactate or fumarate was calculated as substrate produced (acetate or succinate)/substrate consumed (lactate or fumarate) * 100%.
[c]and [d]were calculated according to Equation 5 and 6, respectively, as described in Materials and Methods.
[e]expressed in milligram of biomass formed per mole or C-mole of substrate consumed (mg mol^{-1}).

1 (Table 2). Fumarate appeared to be largely (> 85%) reduced to succinate in all chemostats, but only 55%–62% and 66%–85% of lactate was oxidized to acetate in lactate- and fumarate-limited chemostats respectively (Table 2). For either limitation, metabolic inflexibility should have made growth yields per mole of either substrate independent of the limitation applied. But the growth yield per mole of fumarate consumed was two-fold lower in the lactate-limited chemostats than in two fumarate-limited chemostats F1 and F3 [11 and 8.5 mg biomass $(mol\ fumarate)^{-1}$] respectively (Table 2); in F2 the growth yield per mol of fumarate was similar to that in lactate-limited chemostats. The growth yields per mole of lactate were largely independent of the redox limitation. The carbon and electron recoveries ranged from 80% to 90% for all chemostat runs (Table 2). As batch experiments had not suggested any formation of pyruvate, ethanol, formate or hydrogen gas, their formation was not monitored in chemostats.

Altered transcriptome and proteome upon limitations in chemostats

In the transcriptome, approximately 3454 genes (70% of the 5060 predicted protein-coding genes) were detected to be differentially expressed at least in one of the conditions (Supporting Information Table S2). In the proteome, 825 proteins were identified as such in at least one chemostat (Supporting Information Table S2). The criteria for

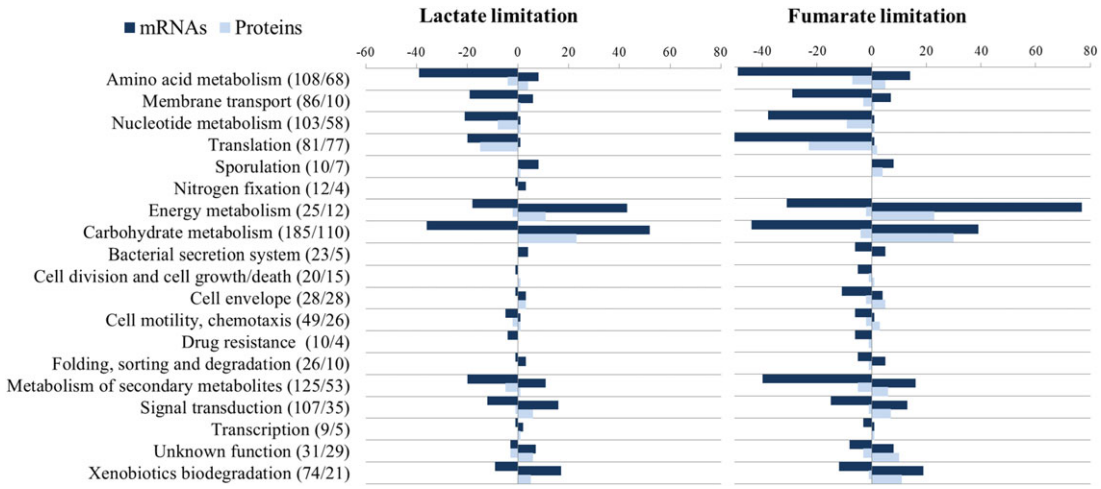

Fig. 1. Number of differentially up- (shown as positive) and down- (shown as negative) regulated mRNAs and proteins clustered according to KEGG categories [with ^{2}log(expression ratio)'s > 1.5 and < −1.5] under fumarate- and lactate-limiting conditions in chemostats relative to batch cultures. Averaged values between biological replicates are presented. Values, which had strongly different regulation between biological replicates or that were detected only once, were filtered out (hence not shown). Total mRNAs/proteins detected within each category are indicated in parentheses.

differential expression was that ^{2}log of the ratios of genes or proteins in chemostats relative to batch were above 1 or below −1 (i.e., the ratios themselves were higher than 2 or lower than 0.5) as observed in at least one of the biological replicates.

Both limiting conditions led to mostly down regulation of mRNAs and proteins of amino acid and secondary metabolites metabolism, membrane transport, nucleotide metabolism and translation (Fig. 1). Under all limiting conditions, there was also an 'anxiety' response: sporulation was the category where most mRNAs and proteins were upregulated (Fig. 1). Microscopic examination confirmed the presence of spores. A number of growth-related proteins from the category cell division, growth and death appeared downregulated (Supporting Information Table S2) with significant downregulation of several genes during fumarate limitation (Fig. 1). Fumarate limitation induced more genes and proteins of energy conservation than the other limitation did (Fig. 1), which included such subcategories as nitrogen metabolism, redox reactions and sulfur metabolism (Fig. 2). Lactate limitation was characterized by the highest number of upregulated mRNAs and proteins assigned to the carbohydrate metabolism category (Fig. 1). The upregulation of carbohydrate metabolism genes under lactate limitation (Fig. 1) and of putative DMSO, sulfite and nitrate/nitrite reductases under fumarate limitation (Fig. 2) may suggest that the organism was searching for alternative carbon or energy sources.

Not just transcription regulation but also regulation at the level of protein synthesis or degradation

We next asked whether the altered gene expression consequent upon limitation could be accounted for by transcriptional regulation only. Although the *average* slope of the correlation between protein and mRNA levels was 1.0 (Supporting Information Fig. S1D), the correlation coefficient (0.5; Supporting Information Fig. S1D) was much lower than the 0.8 observed for the biological replica for mRNAs (Supporting Information Fig. S1B) and proteins (Supporting Information Fig. S1C). Extending hierarchical regulation analysis (Rossell *et al*., 2005) as explained in the Experimental Procedures section, we plotted the net translational regulation versus the net transcriptional regulation for the lactate and fumarate depriving conditions, in Fig. 3A and B respectively. If regulation had been strong and exclusively transcriptional or exclusively translational, all points should have been far out on the abscissa or ordinate respectively. For both limiting conditions, the deviations from the abscissa were substantial for more than 80% of the proteins, indicating substantial translational regulation. Regulation was not exclusively 'net' translational either ('net' referring to the inclusion of regulation of protein synthesis and degradation, and of growth rate affecting the proteins' dilution into daughter cells); deviations from the ordinate were substantial. In all cases there should have been a component of net translational regulation due to the reduced growth rate in chemostats relative to batch, which would have explained an upward regulation by approximately $-^{2}$log (0.3) = 1.7, but few proteins populated the horizontal line at 1.7: regulation appeared to involve both transcription and (net) translation.

Hierarchical regulation coefficients (Rossell *et al*., 2006) quantify the extent to which the protein concentration is regulated at transcription (or at mRNA degradation) rather than at any post-mRNA level (Table 3; Fig. 3). Only, few proteins from carbon and energy metabolism exhibited exclusively transcriptional regulation (transcription regulation coefficients between 80 and 120) (Table 3).

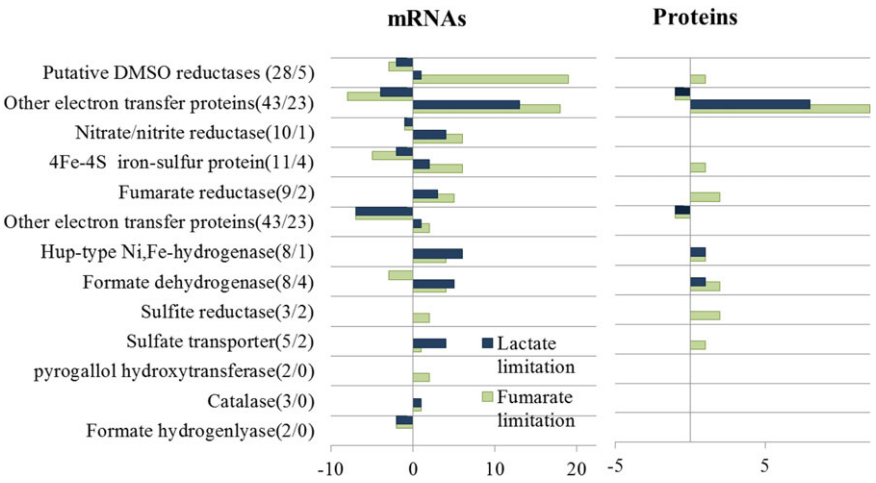

Fig. 2. Number of energy transduction metabolism related differentially up- (shown as positive) and down- (shown as negative) [with ^{2}log(expression ratio)'s > 1.5 or < –1.5] regulated mRNAs and proteins detected in lactate-, and fumarate-limited chemostats. Total mRNAs/proteins detected within each categories are indicated in parentheses.

Intriguingly, for many proteins, transcriptional and translational regulation were in opposite direction (areas 4, –4, 5, and –5 in Fig. 3A), either such that transcription regulation was leading (transcription regulation coefficient > 100%) with translation regulation being homeostatic (translation regulation coefficient < 0) (notably all acetate metabolism and most TCA cycle genes under fumarate limitation), or vice versa where translational regulation was leading (e.g., D-lactate dehydrogenase; DSY2064).

Altered carbon metabolism

Many proteins involved in the expected core carbon metabolism had similar expression patterns for both limiting conditions (Table 3). *D. hafniense* Y51 may have manoeuvred itself into a condition of being limited in terms of both substrates, by also consuming the remainders of the substrate that should have been in excess (according to Process 1). For example, under both limiting conditions lactate permease (DSY2261) was the protein with the strongest upregulation (Table 3). Additionally, although *L*-lactate was fed into chemostats, three *D*-lactate dehydrogenases (DSY2064, DSY3216, DSY3218) increased in abundance when fumarate was made limiting and were regulated at the translational level, suggesting that under both limiting conditions *D. hafniense* Y51 was searching also through translational regulation for alternatives to *L*-lactate.

The genome of *D. hafniense* Y51 does not encode a complete TCA cycle: it encodes the dihydrolipoamide dehydrogenase (DSY2918) of the oxoglutarate dehydrogenase complex but its dihydrolipoyl succinyltransferase and 2-oxogluatarate dehydrogenase are missing, interrupting the TCA cycle. The oxidative branch [citrate synthase (DSY3039), aconitate hydratase (DSY4204) and isocitrate dehydrogenase (DSY3882)] was downregulated under lactate and fumarate limitation. This was possibly related to the decreased growth rates in chemostats relative to batch.

A transcript and a protein of putative aldehyde oxidoreductase (DSY1987) and a transcript of putative iron-containing

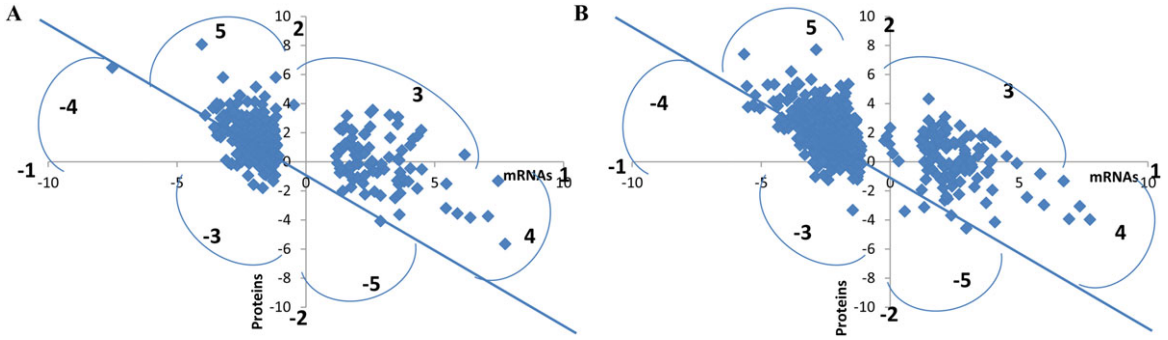

Fig. 3. Protein level regulation versus net transcriptional regulation, when comparing lactate (A) and fumarate (B) limited chemostats with batch growth. As indicated by the numbers in the figures, this regulation analysis enables one to distinguish between 10 categories of regulation: proteins that were regulated through transcription or mRNA degradation only (1 and –1, i.e., points on the abscissa), proteins regulated through translation or protein degradation and dilution due to cell division only (2 and –2, i.e., points on the ordinate), combinations of these two (3 and –3, i.e., the first and third quadrant) as regulations in parallel, and paradoxical combinations of these two (4, –4, 5 and –5, i.e., the second and the fourth quadrant). Proteins depicted above the blue straight line were upregulated while those below that line were down regulated relative to batch growth. For proteins in 4 and –4 area, net transcriptional regulation, dominated over the antiparallel net translational regulation. For proteins in 5 and –5 area, net translational regulation dominated over net transcriptional regulation working in the opposite direction.

Table 3. Differences in expression level of detected mRNAs and of proteins, and coefficients of net transcriptional and net translational regulation (%) related to carbon and energy metabolism in *D. hafniense* Y51, when comparing lactate- and fumarate-limited chemostat cultures with batch culture.

Metabolism	IDs	Annotation	Lactate limitation		Fumarate limitation		Lac. Lim.	Fum lim.	Lac. Lim.	Fum lim.
			2log(ratio)'s				Transcriptional regulation, %		Translational regulation, %	
			mRNAs	proteins	mRNAs	proteins				
Lactate utilization and conversion	DSY1921	Putative Lactate utilization protein B	-1.2	0.4	-1.7	1.1	-270	-150	370	250
	DSY2064	D-lactate dehydrogenase (LutA)	-1.3	1.6	-1.6	2.0	-80	-80	180	180
	DSY2091	Putative lactate dehydrogense (LutA)		3.1	-1.8	2.7		-70		170
	DSY2092	Putative lactate dehydrogense (LutB)		1.1		1.6				
	DSY2261	L-lactate permease	4.1	5.2	4.1	5.4	80	80	20	20
	DSY3216	D-lactate dehydrogenase/gluconate (GlcD)		2.9		3.5				
	DSY3218	Putative D-lactate/gluconate dehydrogenases (GlcF)		2.0	1.4	3.4		40		60
	DSY3357	Putative D-lactate/gluconate dehydrogenases (GlcD)	-2.8	0.2		2.3	-1310		1410	
	DSY3457	Malate/L-lactate dehydrogenase			1.2					
Pyruvate metabolism	DSY0115	Pyruvate oxidoreductase PorA	-2.4	0.5	-3.1	0.9	-490	-350	590	450
	DSY0416	Formate C-acetyltransferase								
	DSY1608	Pyruvate kinase		0.0		0.5				
	DSY3016	Pyruvate-formate lyase	-1.4		-2.2					
	DSY3071	Phosphoenolpyruvate synthase			-1.3					
	DSY3080	Phosphoenolpyruvate synthase	-2.0	2.1	-1.8	1.0	-90	-190	190	290
	DSY4203	Phosphoenolpyruvate carboxykinase (ATP)		-0.1	-1.4	-1.8		80		20
	DSY4262	Pyruvate carboxyltransferase			2.1					
	DSY4274	Phosphoenolpyruvate synthase			-1.3					
	DSY4310	Pyruvate carboxyltransferase	-2.9		-2.9					
	DSY4888	Pyruvate-flavodoxin oxidoreductase PorA	2.7		2.8					
	DSY5006	Formate C-acetyltransferase			2.7					
Acetate metabolism	DSY0515	Acetate/CoA ligase AcsA	5.4							
	DSY0633	Acetyl-CoA hydrolase/transferase			-1.2					
	DSY1315	Acetyl-CoA carboxylase, beta subunit	-1.6	0.3	-2.1	-0.3	-620	700	720	-600
	DSY1316	Acetyl-CoA carboxylase, alpha subunit	-2.2	-0.4	-2.6	-0.5	490	500	-390	-400
	DSY1711	Acetyl-CoA hydrolase/transferase	6.1		2.3					
	DSY2366	Biotin carboxylase	-2.1	-0.3	-3.1	-1.0	640	310	-540	-210
	DSY2367	Acetyl-CoA carboxylase, biotin carboxyl carrier	-3.6	0.1	-4.4	-0.3	-3510	1700	3610	-1600
	DSY2668	Acetate kinase	-2.8	-0.5	-3.1	-0.2	570	1270	-470	-1170
	DSY3366	Acetyl-CoA hydrolase/transferase	5.2		1.5					
Butanoate	DSY2401	Probable butyrate kinase (acetate kinase, Peng et al., 2012)	4.6		2.5					
TCA cycle	DSY1923	Putative malic enzyme (Malate dehydrogenase)		-0.4	1.6	1.1		150		-50
	DSY1924	Citryl-CoA lyase		2.6	1.7	2.6		70		30
	DSY1925	Succinate--CoA ligase (ADP-forming) alpha subunit		-0.9		1.5				
	DSY1926	Succinate--CoA ligase (ADP-forming) beta subunit		-0.2	1.6	1.1		140		-40
	DSY3038	Citrate lyase, alpha subunit	-1.2	-2.1		-0.5	60		40	
	DSY3039	Citrate (Si)-synthase	-1.8	-1.0	-1.8	0.0	180	5560	-80	-5460
	DSY3230	Hydro-lyase, Fe-S type (Fumarase), alpha subunit	1.4	2.2		1.2	60		40	
	DSY3245	Malate dehydrogenase			-1.4					
	DSY3584	Malate dehydrogenase, NAD-dependent								
	DSY3882	Isocitrate dehydrogenase, NADP-dependent	-3.2	-0.6	-3.1	-0.2	540	1720	-440	-1620
	DSY4204	Aconitate hydratase domain protein	-3.3	-0.3	-3.4	-1.0	1080	350	-980	-250
Fumarate reductase paralogs	DSY0735	Succinate dehydrogenase/Fumarate reductase cytochrome b subunit	6.1		3.0					
	DSY0736	Succinate dehydrogenase/Fumarate reductase flavoprotein subunit	5.5		1.9					
	DSY0737	Succinate dehydrogenase/Fumarate reductase iron-sulfur protein	6.0		1.3					
	DSY3139	Putative fumarate reductase flavoprotein subunit		3.6	2.1	4.1		50		50
	DSY0285	Putative fumarate reductase flavoprotein subunit		1.4	1.5	3.5		40		60
	DSY0513	Putative fumarate reductase flavoprotein subunit	2.7		2.3					
	DSY1391	Putative fumarate reductase flavoprotein subunit		1.0	3.8	3.2		120		-20

(Continues)

Table 3. Continued

	DSY1422	Putative fumarate reductase flavoprotein subunit	2.0		4.4					
	DSY1829	Putative fumarate reductase flavoprotein subunit			3.8					
	DSY3728	Putative fumarate reductase flavoprotein subunit			3.7					
Alcohol metabolism	DSY0565	Putative Iron-containing alcohol dehydrogenase	7.7	2.1	6.9	3.0	370	230	-270	-130
	DSY0623	Iron-containing alcohol dehydrogenase	-1.5		-1.5					
	DSY1987	Putative aldehyde oxidoreductase	2.5	4.9	3.7	5.5	50	70	50	30
	DSY2755	Putative Iron-containing alcohol dehydrogenase			1.0					
Wood-Ljungdahl pathway	DSY0138	Methylenetetrahydrofolate reductase		1.7	-2.6	-0.2		1660		-1560
	DSY0205	Formate--tetrahydrofolate ligase	1.8	3.9	1.8	3.2	50	60	50	40
	DSY1648	Carbon monoxide dehydrogenase/acetyl-CoA synthase delta subunit	3.8	2.4	3.1	2.8	160	110	-60	-10
	DSY1649	CO dehydrogenase maturation factor	3.5	1.0	3.3	1.5	360	210	-260	-110
	DSY1650	Ferredoxin	4.3	2.5	3.7	3.0	170	120	-70	-20
	DSY1651	Carbon monoxide dehydrogenase/acetyl-CoA synthase gamma subunit	3.6	2.0	2.9	3.3	180	90	-80	10
	DSY1652	Carbon monoxide dehydrogenase/acetyl-CoA synthase alpha subunit	3.7	4.5	3.1	4.9	80	60	20	40
	DSY1653	Carbon monoxide dehydrogenase/acetyl-CoA synthase beta subunit	4.1	3.6	3.9	4.1	110	100	-10	0
	DSY1654	CO dehydrogenase maturation factor	3.7	1.5	2.6	2.0	240	130	-140	-30
	DSY2356	Methylene-THF dehydrogenase	1.3	2.2		1.2	60		40	
	DSY2630	Carbon-monoxide dehydrogenase	-1.4							
	DSY2631	Carbon monoxide dehydrogenase maturation factor	-1.8							
	DSY3972	5-formyltetrahydrofolate cyclo-ligase (EC 6.3.3.2)	1.3		2.2					
	DSY4173	Carbon-monoxide dehydrogenase	2.4		2.9					
	DSY4442	Carbon-monoxide dehydrogenase	2.0	3.0	2.5	3.8	70	60	30	40
Hydrogenases	DSY0794	Hup-type Ni,Fe-hydrogenase cytochrome b subunit	1.8		2.2					
	DSY0795	Nickel-dependent hydrogenase large subunit	2.3							
	DSY0796	Hup-type Ni,Fe-hydrogenase small subunit	2.1		1.7					
	DSY0803	Putative hydrogenase large subunit domain protein	2.3		2.1					
	DSY1596	Ni,Fe-hydrogenase maturation factor	3.2							
	DSY1597	Hup-type Ni,Fe-hydrogenase cytochrome b subunit	3.2		-4.0					
	DSY1598	Hup-type Ni,Fe-hydrogenase large subunit	3.6	6.1	-2.9	1.9	60	-160	40	260
	DSY1599	Hup-type Ni,Fe-hydrogenase small subunit	2.9		-3.6					
	DSY2100	Nickel-dependent hydrogenase large subunit			2.0					
	DSY2101	Ni,Fe-hydrogenase small subunit			1.9					
	DSY2238	Hup-type Ni,Fe-hydrogenase small subunit	2.9		2.3					
	DSY2239	Hup-type Ni,Fe-hydrogenase large subunit	2.4		1.9					
	DSY2240	Hup-type Ni,Fe-hydrogenase cytochrome b subunit	2.3		2.3					
	DSY3114	Formate hydrogenlyase subunit 7	-3.3		-3.4					
	DSY3115	NADH dehydrogenase (quinone) (EC 1.6.99.5)	-3.1		-3.1					
	DSY3116	Hydrogenase-4 component F	-2.5		-2.2					
	DSY3117	Hydrogenase-4 component E	-3.7		-3.5					
	DSY3118	Formate hydrogenlyase subunit 4	-3.6		-3.6					
	DSY3119	Hydrogenase-4 component B	-2.9		-3.2					
	DSY4326	Putative hydrogenase large subunit domain protein	-2.0	-3.6	-2.4	-3.6	60	70	40	30
	DSY4711	Putative hydrogenase iron-sulfur subunit	-4.2		-3.8					
	DSY4712	Putative hydrogenase large subunit	-4.4		-4.4					
Formate metabolism	DSY3098	Formate dehydrogenase (quinone-dependent), membrane-bound	4.3	6.1	-1.7		70		30	
	DSY3099	Formate dehydrogenase (quinone-dependent), membrane-bound	3.7		-1.5					
	DSY3100	Formate dehydrogenase (quinone-dependent) , membrane-bound	3.7		-2.5					
	DSY3101	Formate dehydrogenase, alpha subunit (quinone-dependent), (DSMO red.)	2.8		-1.7					
	DSY3526	Formate dehydrogenase			2.2					
	DSY3896	Formate dehydrogenase		-5.2	2.9	3.5		80		20
	DSY3968	Formate dehydrogenase, alpha subunit (NAD-dependent) (DSMO reductase) (cytoplasmic)	2.3	4.2	1.7	3.4	60	50	40	50
	DSY3969	NADH dehydrogenase I chain (cytoplasmic)	1.5	4.0	1.5	4.3	40	30	60	70
	DSY3970	NADH dehydrogenase (quinone) (cytoplasmic)		3.2	-3.1	2.6		-120		220
	DSY3971	NADH dehydrogenase I chain E (EC 1.6.5.3)	2.0	2.5	1.9	2.0	80	100	20	0

Regulation coefficients (%) were calculated as described under section on 'Experimental procedures'. ^{2}log(ratio)'s of chemostat values relative to batch with coefficient of variation (CV) below 51%, were used for the heatmap with colours ranging from: −3.9 to 7.7.

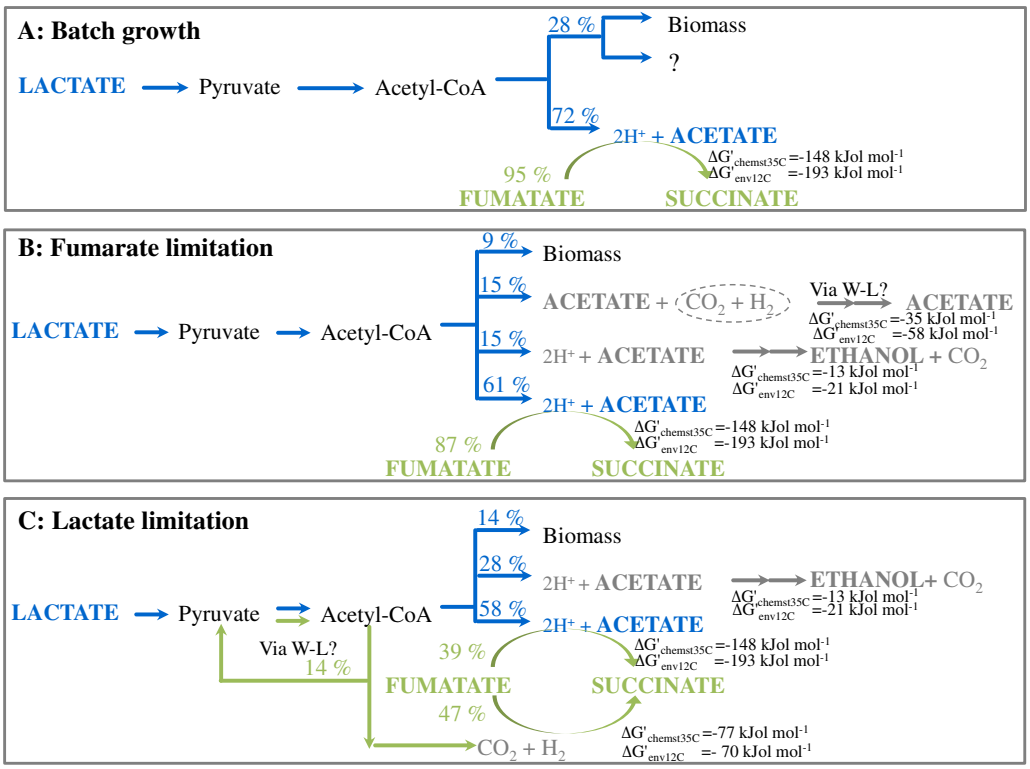

Fig. 4. Schematic representation of proposed main metabolic reactions under the three growth conditions: A—batch, B—fumarate limitation and C—lactate limitation. Estimated predicted processes from Table 1 are indicated next to a range of estimated fluxes through them (Supporting Information Table S3). Blue colour represents fluxes from lactate. Green colour represents fluxes from fumarate. Grey colour represents the substrates which were not measured but were expected to be formed. Calculation for percentage of fluxes is based on flux analysis (Supporting Information Table S3). W–L refers to the Wood–Ljungdahl pathway.

alcohol dehydrogenase (DSY0565) had high ^{2}log(ratio)'s (of up to 8): they strongly increased in expression under both lactate and fumarate limiting conditions (Table 3). This suggests that ethanol metabolism might play an important role under both limiting conditions.

The main difference in carbon metabolism between lactate and fumarate limitation was strong upregulation under lactate limitation of all possible acetate production/consumption proteins [acetate-CoA ligase (DSY0515), CoA/hydrolases (DSY1711, DSY3366) and butyrate kinase (DSY2401), membrane-bound succinate dehydrogenase/fumarate reductase (DSY0735–0737)] (Table 3) and transport of C4-dicarboxylates (TRAP transporters, Supporting Information Table S2).

Proteins and mRNAs of the Wood–Ljungdahl pathway showed the most pronounced coordinated response to the metabolic limitations, as induction orchestrated at the transcription level (Table 3). In particular, methylene-tetrahydrofolate dehydrogenase (DSY2356), formate-tetrahydrofolate ligase (DSY0205), and carbon monoxide dehydrogenases (DSY1648–1654; DSY4442) were upregulated under all limiting conditions (Table 3). Although the Wood–Ljungdahl pathway has been shown to be involved into utilization of phenyl methyl ethers (Mingo *et al*., 2014), in our experiments O-demethylase/methyltransferase genes were not detected.

Energy transduction

Fumarate limitation produced stronger upregulation of energy transduction than lactate limitation. Many genes expressed were related to reduction of alternative electron acceptors (putative DMSO reductases, nitrate/nitrite and sulfite reductases) (69 transcripts) (Fig. 2).

The genome of *D. hafniense* Y51 encodes four Ni,Fe-hydrogen uptake hydrogenases (DSY1597–1599; DSY0794–0796; DSY2238–2240; DSY2100–2101), a hydrogenase complex (DSY3116–3119) associated with putative formate hydrogen lyase (DSY3114–3115), and Fe-hydrogenases (DSY0803; 4326; 4711–4712; 0936) (Vignais and Billoud, 2007). These genes were sometimes subject to limitation-specific regulation (Table 3). Transcripts of Ni,Fe-hydrogen uptake hydrogenase DSY1597–1599 were upregulated only under lactate limitation, whereas other hydrogen-producing hydrogenases were either upregulated under all conditions (DSY0794–0796, DSY2238–2240), or only upon fumarate limitation (DSY2100–2101) (Table 3). Hydrogen-

evolving Fe-hydrogenases were either not significantly upregulated (DSY0803) or significantly downregulated (DSY4326, DSY4711–4712) (Table 3). The formate hydrogen lyase complex DSY3114–3115 was downregulated under all limiting conditions (Table 3). Although the role of this complex in D. hafniense Y51 is still unclear (Kruse *et al.*, 2017), it seems to play a role during exponential growth in batch and might be repressed in chemostats.

About 8 of the 31 predicted fumarate reductase paralogs (DSY3139; DSY0285, DSY3728; DSY0513; DSY1391; DSY1422; DSY1829), including a canonical fumarate reductase DSY0735–0737 (Kruse *et al.*, 2017), as well as formate dehydrogenases DSY3098–3101, DSY3526, DSY3896 and DSY3968–3971, were detected by combined proteomic and transcriptomic analysis (Table 3). Transcripts of membrane-bound canonical fumarate reductase DSY0735–0737 were found to be upregulated under lactate limitation only (Table 3).

Discussion

At excess of substrates in batch, *D. hafniense* Y51 grows essentially in accordance with the predicted stoichiometry for lactate/fumarate redox reaction. In contrast, during continuous cultivation at 0.02 h^{-1} dilution rate, *D. hafniense* Y51 adjusts its metabolism as if trying to benefit fully from the excess of substrates (Table 2). As no monitoring of alternative products for lactate conversion (such as H_2 and ethanol) was carried out in the current study, we combined flux analysis (Supporting Information Table S3), thermodynamics (Supporting Information Table S4), and proteomic and transcriptomic data in order to achieve plausible explanations for metabolic rerouting under substrate limiting conditions. Our interpretation is that the organism is metabolically versatile and under limiting conditions does not need to adhere to the metabolic behaviour (Process 1) it uses in batch during substrate excess.

Lactate utilization

Although the fumarate in fumarate-limited chemostats sufficed to oxidize only 60%–75% of the inflowing lactate, 100%–83% of the lactate was in fact consumed (chemostats F1–F3 in Table 2). In the absence of electron acceptors, many bacteria can ferment lactate while producing hydrogen, acetate and CO_2 and/or propionate as the products (Gottschalk, 1986), but neither *D. hafniense* Y51 nor its homologous strain DCB-2 has been reported to grow fermentatively on lactate (Christiansen and Ahring, 1996; Suyama *et al*., 2001; Nonaka *et al*., 2006; Peng *et al*., 2012). However, in our batch experiments, some 28% (4.8 mM) of the lactate was not recovered in the form of the acetate as was expected according to Process 1 (Fig. 4A). Since that much lactate could not have ended up in the biomass, we wondered whether that unrecovered lactate might have been fermented.

To examine possible fermentation pathways, we estimated their Gibbs energies (Supporting Information Table S4). We did this in terms of a 'chemostat-standard Gibbs energy difference' ($\Delta G'_{chemst}$). This takes as the standard state not the usual 1 Molar concentrations and 1 atm pressure, but the smaller concentrations and partial pressures that are more relevant for chemostat conditions. For lactate fermentation (Fig. 4B and C) into ethanol and carbon dioxide, we calculated $\Delta G'_{chemst}$ = –13 kJ mol^{-1} (Process 3) and for lactate fermenting into acetate, carbon dioxide and hydrogen $\Delta G'_{chemst}$ = –35 kJ mol^{-1} (Process 4; Table 1; for other possible fermentation pathways refer to Supporting Information Table S4). This suggests that fermentation into ethanol and CO_2 was a thermodynamic option. As 15% and 28% of the lactate consumed in lactate- and fumarate-limited chemostats, respectively, was recovered neither as acetate nor as biomass (Table 2) and strong upregulation of mRNAs and proteins of ethanol metabolism were observed (Table 3), we speculate that this lactate may have been fermented into ethanol in both limiting conditions. Under fumarate limitation production of ethanol could be a plausible strategy to consume reducing equivalents.

The production of acetate, CO_2 and H_2 (Process 4) in fumarate-limited chemostats might also be possible as some hydrogenases were upregulated (Table 3). Our continuous flushing of the chemostat with N_2/CO_2 may have kept the hydrogen partial pressure low enough for the reaction to be carried out (as estimated by the negative $\Delta G'_{chemst}$ = –35 kJ mol^{-1}; see section on 'Experimental procedures').

Since much of the Wood-Ljungdahl pathway was also upregulated, it may have been involved in the recycling of redox equivalents deriving from fermentation. From an energetic point of view, although $\Delta G'_{chemst}$ of processes 3 and 4 is below the Gibbs energy required for ATP synthesis, Gibbs energy might still be harvested if a corresponding coupling mechanism was available. Bacterial cells would anyway not be washed out as lactate oxidation via fumarate reduction would be the prevailing process with 61% of lactate directed into it under fumarate limitation, thereby providing substantial Gibbs energy for growth (Fig. 4B), with perhaps some extra proton motive force generated via processes 3 and 4. Moreover, the predicted processes for utilization of lactate were estimated with 100% prediction (Supporting Information Table S3).

Disproportionation of excess fumarate under electron donor limitation?

A plausible explanation for the absence of residual fumarate in the outflow under lactate limitation is that part of

the surplus fumarate was oxidized to CO_2 with the released electrons being used to reduce the rest of the fumarate to succinate ($\Delta G'_{chemst}$ = −55 kJ mol^{-1} fumarate used): 7 molecules of fumarate would be disproportionated to 6 molecules of succinate and 4 molecules of carbon dioxide ($\Delta G'_{chemst}$ = −387 kJ mol^{-1}; Process 2 in Table 1). As reduction of fumarate to succinate via lactate oxidation to acetate yields more Gibbs energy per mole of fumarate ($\Delta G'_{chemst}$ = −148 kJ mol^{-1} fumarate used; Process 1), fumarate disproportionation might be expected to be switched on when all lactate has been consumed via Process 1. The amount of acetate produced corresponded to approximately 39% of the fumarate being reduced to succinate (Fig. 4C). The amount of fumarate not recovered in the form of succinate was 14% (8–9 mM) of the fumarate consumed and would have sufficed to produce redox equivalents for the reduction of the rest (47%) of the fumarate (Fig. 4C).

Fumarate disproportionation has been described earlier for other bacteria (Kroger, 1974; Plugge *et al*., 1993; Zaunmuller *et al*., 2006; Plugge *et al*., 2012). Fumarate can be either hydrated to malate (Zaunmuller *et al*., 2006; Zhang *et al*., 2011) or completely oxidized via the reverse Wood-Ljungdahl pathway with the production of 4 CO_2 and 12 reducing equivalents (Plugge *et al*., 2012). As no genes for fumarate hydration were upregulated under lactate limitation, we suggest that the acetyl-CoA produced by *D. hafniense* Y51 from the oxidation of fumarate was being fed into the reverse Wood–Ljungdahl pathway with consequent production of redox equivalents and carbon dioxide (Fig. 4C). These redox equivalents would then be used to reduce more fumarate to succinate (as part of Process 2). The reverse operation of the formate-tetrahydrofolate ligase (DSY0205) (Table 3) should be expected to produce ATP, which has a Gibbs energy relative to ADP and phosphate of approximately 48 kJ mol^{-1} (Westerhoff and Van Dam, 1987). Sufficient thermodynamic power for this would come from Gibbs free energy made available by the overall fumarate disproportionation reaction (Supporting Information Table S3). Similarly, sulfate-reducing bacteria also use the reverse Wood–Ljungdahl pathway and carry out the endergonic reaction of acetate conversion to H_2 and CO_2 via coupling to the exergonic reaction of sulfate reduction (Ragsdale and Pierce, 2008).

The reverse operation of the Wood–Ljungdahl pathway is suggested by the strong upregulation of the membrane-bound formate dehydrogenase (DSY3098–3101) only under lactate limitation (Table 3). This enzyme enables the conversion of formate into redox equivalents and CO_2 (Kim *et al*., 2012). A recent study by (Kruse *et al*., 2015) showed that in *D. dehalogenans* electron transfer from formate to fumarate is carried out by the membrane-bound formate dehydrogenase in a complex with quinone-dependent succinate dehydrogenase/fumarate reductase DSY0735–0737. Interestingly, the latter enzyme is not induced by *D. hafniense* Y51 in the presence of fumarate and formate (Peng *et al*., 2012). Therefore, fumarate reductase DSY0735–0737 is not induced by fumarate itself but may play a role in the electron transfer chain under some conditions. We suggest that under electron donor limiting conditions reduction of excessive fumarate to succinate may be carried out by a formate dehydrogenase – succinate dehydrogenase/fumarate reductase complex.

Extensive and varied regulation of metabolism

How does *D. hafniense* Y51 regulate its metabolism when confronted with limitations? In the absence of alternative external electron donors and acceptors, this is not immediately obvious. The metabolic rerouting should be consistent with thermodynamics and likely have led to volatile or unstable products that we were not able to measure. And it should require metabolic rewiring, that is, activation of different metabolic pathways. Metabolic rewiring can be affected by metabolic, translational or transcriptional regulation, where the latter two should be reflected by differential changes in mRNA and protein levels, or just changes in mRNA levels respectively (Rossell *et al*., 2006). Many net translation-regulation coefficients were positive between 0% and 100%, but some exceeded 100% (hyper regulation at the net translation level) or were negative (counter regulation at the net translation level). At the same time, there was a diverse pattern of transcription regulation with many genes significantly regulated. Remarkably, *D. hafniense* Y51 did not merely adjust its metabolism by re-tuning transcription of a few genes encoding enzymes with high flux control, nor did it engage in proportional regulation (Rossell *et al*., 2006, 2008); it appeared to re-tune its metabolism in a variety of more subtle ways.

Adaptive response to limiting conditions in chemostats: A shift to an exploratory mode?

The investigation of the physiology of *D. hafniense* Y51 under limiting conditions in chemostats showed that this strain exhibits an extraordinarily flexible metabolic potential as expressed at the mRNA and protein levels. This enabled it to switch between reduction–oxidation reactions and fermentation. Under fumarate limiting conditions, it fermented lactate whereas under lactate limiting conditions it appeared to disproportionate fumarate, and in either case was able to make use of excess substrate.

Other organisms under limitations in chemostats or retentostats are known to release carbon catabolite repression which then leads to upregulation of degradation pathways of alternative substrates which are not present in the medium (Franchini and Egli, 2006; Trautwein

et al., 2012; Marozava *et al*., 2014; Overkamp *et al*., 2015). The first study on *D. hafniense* Y51 in batch (Suyama *et al*., 2001) showed that *D. hafniense* Y51 can grow on pyruvate, lactate, and formate as carbon sources but not on other carbon substrates such as succinate, acetate, ethanol and malate. However, studies establishing whether *D. hafniense* Y51 exhibits a carbon catabolite repression that is relieved by substrate limitation in chemostats have been lacking. Our observations could reflect such repression. Alternatively, the above-listed compounds may be important metabolites of adaptive bacterial physiology during electron donor limitation. Under such limitation *D. hafniense* Y51 may adapt to utilization of available substrates and even to substrates that are absent: that is, it may go into an exploratory mode. During fumarate disproportionation, substantial amounts of protons are pumped and released which might explain upregulation of alcohol dehydrogenases; production of some ethanol would consume protons. Furthermore, a formate dehydrogenase–succinate dehydrogenase/fumarate reductase complex may be involved in the reduction of excessive fumarate during fumarate disproportionation. Upregulation of acetyl-CoA transferase/hydrolases (DSY1711 and DSY3366) under lactate limitation might suggest induction of acetate excretion independent from substrate-level phosphorylation which might show the tendency to harvest Gibbs energy through proton motive force under limiting conditions.

Electron acceptor limitation has also been shown to trigger expression of alternative pathways (Bansal *et al*., 2013). In the present study, *D. hafniense* Y51 exhibited upregulation of many unexpected mRNAs and proteins related to utilization of alternative electron acceptors such as DMSO, sulfate and nitrate. The concurrent expression of genes for alternative acceptors suggests that *D. hafniense* Y51 can use a variety of substrates if available in its environment. This makes the organism robust and able to persist and even grow during times where the most ideal substrates for growth are not available.

The present study has focused on the potential of *D. hafniense* Y51 for a versatile metabolism through strong regulation of a variety of metabolic pathways at both the transcriptional and the translational level. This potential versatility is so extensive that further work is needed to establish whether the organism can actually use it when confronted with the many corresponding substrates under the actual conditions relevant for bioremediation. The conditions that we used in this study were a compromise between immediate relevance for bioremediation in the environment, and more academic conditions required to draw pertinent conclusions from the data with respect to regulation. We are able to show that *D. hafniense* Y51 can do more than the stoichiometric reduction of an electron acceptor by lactate; it readily made use of the superstoichiometric excess of either the electron donor or the electron acceptor. We conclude that *D. hafniense* Y51 may offer great potential for bioremediation of PCE-polluted groundwater and sediments, by nature of its robustness and metabolic flexibility, both related to the fact that it tends to readily rewire its metabolism.

Experimental procedures

Cultivation of D. hafniense *Y51 in batch cultures*

D. hafniense strain Y51 was kindly provided by Prof. Dr. Masatoshi Goto, Department of Bioscience and Biotechnology, Faculty of Agriculture, Kyushu University, Japan. Strain Y51 was cultivated anaerobically under a N_2/CO_2 atmosphere (90:10) in a modified *Desulfitobacterium hafniense* DSMZ medium 720, containing (per litre): 1.0 g NH_4Cl, 0.4 g K_2HPO_4, 0.1 g $MgSO_4 \cdot 7H_2O$, 1 ml resazurine stock solution (0.5% w/v), 1 ml DSMZ trace element solution (SL-10), 1 ml DSMZ selenite-tungstate solution, 0.01% yeast extract and cysteine as an oxygen scavenger (0.8 mM). Sodium L-lactate (20 mM) and sodium fumarate (25 mM) were used as electron donor and acceptor respectively (batches B1 and B2, Table 2). The medium was dispensed into 1 l serum bottles, sealed with butyl rubber stoppers and autoclaved at 121 °C for 15 min. After cooling, 30 ml bicarbonate (1.0 M) solution (pH 7.0 $\pm$ 0.2), 1 ml vitamin solution (DSMZ medium 141), 1 ml vitamin cobalamine-B_{12} (5 mg per 100 ml) and 1 ml $CaCl_2$ stock solution (0.3 M) were added to the medium yielding 1 l in total. Bottles were inoculated with 1% (v/v) pre-culture and incubated in duplicate at 35°C in the dark. Bacterial cells for transcriptomic and proteomic analysis were harvested during the early exponential growth phase (at approximate concentration of 9×10^7 cells ml^{-1}).

Cultivation of D. hafniense *Y51 in chemostats*

The chemostat set-up was built by the electronics and mechanics workshops of the Faculty of Earth and Life Sciences, VU University Amsterdam, the Netherlands as previously described (Stouthamer and Bettenhaussen, 1975). The fermenter vessels, operated after sterilization, had a working volume of 1 l, were stirred at 330 rpm and maintained at 35°C. The pH (7.0 $\pm$ 0.2) was controlled by the addition of 1 M HCl or NaOH. A gas mixture of N_2 and CO_2 (95:5) was flushed through the culture at 2 l h^{-1}. Traces of oxygen in the gas mixture were removed by flushing it first through a titanium(III)-citrate solution (Zehnder, 1989). The gas outlet was connected to a water-filled column, which produced a slight overpressure to avoid leakage of oxygen into the fermenter. The

dilution rate for all chemostats was set to 0.02 h^{-1}. Both fermenter and medium reservoir were kept dark by wrapping with aluminium foil.

The medium for continuous cultivation was identical to the medium used for batch cultures except that in order to achieve electron donor- or electron acceptor-limiting conditions, concentrations of the respective nutrients were adjusted. Oxidation of lactate ($C_3H_5O_3^-$) to acetate ($C_2H_3O_2^-$) and carbon dioxide (CO_2) with fumarate ($C_4H_2O_4^{2-}$) as electron acceptor yielding succinate ($C_4H_4O_4^{2-}$) in aqueous solution was expected to follow Process 1 (Table 1). For electron donor-limiting conditions the molar ratio of fumarate to lactate applied through the feed was 3 (60 mM fumarate to 20 mM lactate; for two independent chemostat runs called L1 and L2). For electron acceptor-limited growth the ratio was 1.5, 1.3 and 1.2 (30, 25 and 35 mM fumarate to 20, 20 and 30 mM lactate respectively) for three independent chemostat runs F1, F2 and F3 respectively (Table 2).

Chemostats were inoculated with 10% (v/v) pre-culture. After operating in a batch mode for 2 days when nearly all lactate or fumarate was consumed, the fermenter was switched to chemostat mode. The operating conditions were constant for at least five volume changes to achieve steady state, after which the chemostat was sampled for quantification of biomass, fermentation products and for transcriptomic and proteomic analysis.

Analytical measurements

Optical densities of liquid cultures as proxy of bacterial biomass were measured at a wavelength of 600 nm. Cell numbers were determined with a Multisizer 3 Coulter Counter (Beckman Coulter, CA). Dry weight was measured as previously described (Van Verseveld *et al*., 1984). Organic acids were measured by HPLC (LC-10AT, Shimadzu, Kyoto, Japan) on a packed Aminex-HPC 87H column (300 × 7.8 mm; Biorad Laboratories, Hercules, CA), and a refractive index detector (RID-10A, Shimadzu, Kyoto, Japan) according to (Rossell *et al*., 2008). Although chemostat cultivations were carried out under sterile conditions, the purity of *D. hafniense* Y51 was confirmed microscopically by cultivation on LB agar plates under oxic conditions and by PCR amplification of 16S rRNA gene fragments with generic primers for bacteria followed by Denaturing Gradient Gel Electrophoresis (DGGE), as previously described (Direito *et al*., 2011).

Gibbs energy calculations

Gibbs energies of formation cited by (Thauer *et al*., 1977) were used. Computed reaction Gibbs free energy differences were checked for consistency with results in that study. $\Delta G'_0$ is the Gibbs free energy of reaction in the standard state of 1 atm (100,000 Pa) partial pressure for all gases, 1 M activity (concentration) of all solutes, pH = 7.0, and 55 M for water. In Biology gases are often below 0.01 atm, and solutes often below 5 mM. We therefore rewrite the expression for the Gibbs energy change of reaction:

$$\Delta G = \Delta G'_{\text{envst}} + R \cdot T \cdot \ln\left(\frac{[P]}{[P]_{\text{envst}}} \cdot \frac{[S]_{\text{envst}}}{[S]}\right) \cong \Delta G'_{\text{envst}} \quad (1)$$

With for Gibbs energy drop of reaction at the standard state for the environment:

$$\Delta G'_{\text{envst}} = \Delta G'_0 \frac{\Delta G'_0 - \Delta H'_0}{T} \cdot \delta T + RT \ln\left(\frac{[P]_{\text{envst}}}{[S]_{\text{envst}}}\right) \quad (2)$$

Likewise, for the chemostat:

$$\Delta G = \Delta G'_{\text{chemst}} + R \cdot T \cdot \ln\left(\frac{[P]}{[P]_{\text{chemst}}} \cdot \frac{[S]_{\text{chemst}}}{[S]}\right) \cong \Delta G'_{\text{chemst}} \quad (3)$$

$$\Delta G'_{\text{chemst}} = \Delta G'_0 + \frac{\Delta G'_0 - \Delta H'_0}{T} \cdot \delta T + RT \ln\left(\frac{[P]_{\text{chemst}}}{[S]_{\text{chemst}}}\right) \quad (4)$$

Here δT equals the difference between temperature at the relevant condition (at 12 or 35°C for environment and chemostat respectively) and temperature at standard conditions (25°C); T equals temperature at standard condition in Kelvin (298 K at 25°C). In the supplemental file '$T_{\text{compensation}}$', we show the rationale for the temperature compensation. The 'envst' refers to the new standard state that we here define, that is, the state close to *D. hafniense* in the environment. The standard activities for $\Delta G'_{\text{envst}}$ and $\Delta G'_{\text{chemst}}$ are indicated in Table 4. For $\Delta G'_{\text{chemst}}$ we have used partial pressure of H_2 as 400 Pa because the maximum concentration of H_2 that could build up in our chemostats is predicted to be 15 mM (in the reaction of lactate fermentation into acetate, CO_2 and H_2 in chemostat F3); this amount would be equal approximately to 400 Pa when taking into account the temperature of cultivation (35°C), the flow rate of the inflow gas mixture (0.02 l h^{-1}) and the volume of reactor (2 l).

Table 4. Standard activities taken for calculations of Gibbs energies.

Standard activities	$\Delta G'_{\text{envst}}$	$\Delta G'_{\text{chemst}}$
t, (C°)	12	35
H_2, (Pa)	20*	400
CO_2, (Pa)	40*	5000
HCO_3^-, (mM)	5*	30
Organic molecules, (mM)	0.1*	0.1
Produced organic molecules, (mM)		20

*Represents values taken from Conrad *et al*. (1986).

Determination of physiological parameters

Carbon in the yeast extract was assumed to be completely used for biomass production (4.1 mM, calculated using the molecular formula for yeast extract $CH_{1.9}O_{0.45}N_{0.25}$ (24.6 g $Cmol^{-1}$ molecular mass) (Von Stockar and Liu, 1999). The molecular composition of *D. hafniense* biomass was calculated using molecular formula $CH_{1.8}O_{0.5}N_{0.2}$ (24.6 g $Cmol^{-1}$ molecular mass) (Von Stockar and Liu, 1999).

We assumed that the excess of biomass formed (> 4.1 mM) derived from lactate. Hence, recovery of total carbon (Crectot %) and total electrons (erec %) was calculated according to Process 1 as:

$$\text{Crectot}\% = \frac{2*[\text{Acetate}] + [CO_{2\text{prod}}] + 4*[\text{succinate}] + [\text{Biomass}]}{3*[\text{Lactate}] + 4*[\text{fumarate}] + [\text{Yeast extract}]} \times 100\% \quad (5)$$

$$\text{erec}\% = \frac{8*[\text{Acetate}] + 0*[CO_{2\text{prod}}] + 4.2*[\text{Biomass}] + 14*[\text{Succinate}]}{12*[\text{Lactate}] + 4.25*[\text{Yeast extract}] + 12*[\text{Fumarate}]} \times 100\% \quad (6)$$

where, all concentrations are given in mM, with [Biomass] and [Yeast extract] being given in mM carbon (CmM).

CO_2 could not be determined (due to experimental conditions where CO_2 was present in the nitrogen/CO_2 mixture flushed through the medium to sustain anaerobic conditions). Hence $CO_{2_{\text{prod}}}$ was assumed to equal the measured acetate concentration for the case of Process 1 (Table 1). In Equations 5 and 6, [Lactate] and [Yeast extract] are the respective concentrations of lactate and yeast extract consumed, and [Fumarate] and [Succinate] are the concentrations of fumarate consumed and succinate produced [mM] respectively. Coefficients in Equations 5 and 6 indicate the formal carbon oxidation states in the corresponding compounds respectively.

Growth yield on a given substrate (Y in mg dry weight mol $substrate^{-1}$) was calculated as:

$$Y = \frac{X}{S_0 - S} \quad (7)$$

where, X is the biomass (mg dry weight l^{-1}), S_0 is the substrate concentration of lactate or fumarate [mM] in the chemostat feed (or the total Carbon concentration including that of the yeast extract in CmM) and S is the respective substrate concentration in the outflow [mM].

Hierarchical regulation analysis

For all transcripts that could be detected both in batch and in chemostat experiments, we assessed the changes in mRNA levels in terms of the 2-based logarithm of the ratio of the mRNA level measured in the chemostat relative to the mRNA level measured in batch during fully exponential growth. We did the same for the protein levels. For each detectable protein with a detectable corresponding mRNA we assessed the fraction regulation of the protein concentration at the transcription or mRNA degradation level as the ratio of the logarithm of the ratio-change in mRNA level to the logarithm of the ratio-change in protein level. This fraction corresponds to the coefficient of mRNA level regulation of protein concentration defined by Rossell *et al*. (2006). We extended the Hierarchical Regulation Analysis methodology (Ter Kuile and Westerhoff, 2001; Rossell *et al*., 2005, 2006) by also identifying the non-normalized regulation at the translation/protein degradation level. Assuming protein levels (P) to have attained steady state, there should be a balance of protein synthesis and degradation plus dilution through cell growth:

$$k_{ps} \cdot R = (k_{pd} + \mu) \cdot P \quad (8)$$

Here R and P refer to the mRNA and protein concentrations, respectively, corresponding to any given gene. The μ, k_{ps} and k_{ps} refer to specific growth rate, the rate constant of protein synthesis and the rate constant of protein degradation respectively. The combined regulation by protein synthesis, degradation and dilution due to growth can be found by taking differences of logarithms between chemostat and batch culture:

$$\Delta \ln\left(\frac{k_{ps}}{k_{pd} + \mu}\right) = \Delta \ln P - \Delta \ln R \quad (9)$$

We refer to this combined regulation through changes in $\frac{k_{ps}}{k_{pd} + \mu}$, as protein-level regulation or net translation

regulation, and to the term $\Delta \ln R$ as net transcription regulation. Division by the change in log(protein concentration), shows that regulation of the concentration of a protein can be partly transcriptional and partly at the level of protein metabolism:

$$\rho_{\text{p, transcription}} + \rho_{\text{p, protein level}} = 1 \quad (10)$$

with:

$$\rho_{\text{p,transcription}} \overset{def}{=} \frac{\Delta \ln R}{\Delta \ln P}$$

$$\rho_{\text{p,translation}} \overset{def}{=} \frac{\Delta \ln k_{\text{ps}}}{\Delta \ln P}$$

$$\rho_{\text{p,degradation + dilution}} \overset{def}{=} \frac{\Delta \ln \left(k_{\text{pd}} + \mu\right)}{\Delta \ln P}$$

We report the regulation coefficients $\boldsymbol{\rho_{\text{p,transcription}}}$ and $\boldsymbol{\rho_{\text{p,protein level}}}$ as percentages of total regulation of protein concentration.

$$\boldsymbol{\rho_{\text{p,protein level}} \overset{def}{=} \frac{\Delta \ln k_{\text{ps}} - \Delta \ln \left(k_{\text{pd}} + \mu\right)}{\Delta \ln P} = \rho_{\text{p,translation}} - \rho_{\text{p,degradation + dilution}}} \quad (11)$$

RNA isolation, cDNA synthesis and microarray assays

Samples (100 ml) were taken from the batch cultures or chemostats and immediately mixed with ice-cold methanol (1:1). Then, cells were harvested by centrifugation at 4000*g* for 10 min at 4°C and stored at –80°C until further analysis. Total RNA was isolated from the frozen pellet using a modified version of the Macaloid based RNA isolation protocol (Zoetendal *et al*., 2006). For each sample, a frozen pellet was resuspended in 1 ml ice-cold TE buffer then centrifuged at 10,000*g* for 1 min at 4°C. Supernatant was removed. Afterward, the cell pellets were resuspended in 500 µl ice-cold TE buffer, and the suspension was transferred into 2 ml Macaloid tubes followed by addition of 50 µl Ambion® 10% SDS (Applied BiosystemsTM, Carlsbad, CA) and 500 µl UltraPureTM phenol: water (3.75:1, v/v) (InvitrogenTM, Carlsbad, CA). The samples were treated thrice in a FastPrep®-24 (MP Biomedicals, Solon, OH) at a speed of 5.5 m s^{-1} for 40 s and chilled on ice for 90 s between each FastPrep step. Afterward, the samples were centrifuged at 10,000*g* for 15 min at 4°C, and the upper aqueous phase was transferred into 2 ml pre-centrifuged (16,000*g*, 1 min) Phase Lock Gel Heavy (PLGH) tubes (5 PRIME GmbH, Hamburg, Germany). An equal volume of UltraPureTM phenol:chloroform:isoamyl alcohol (25:24:1, v/v; InvitrogenTM, Carlsbad, CA) was pipetted into each pre-centrifuged PLGH tube. The contents were mixed well and centrifuged at 10,000*g* for 5 min at 4°C, and the supernatant in each tube was transferred into a new PLGH tube. The last three steps were repeated twice or thrice until a clear interface was obtained. Afterward, the supernatant was transferred into a new PLGH tube, and an equal volume mixture of chloroform: isoamyl alcohol (24:1, v/v) (Sigma-Aldrich® chemie GmbH, Steinheim, Germany) was added. The contents were mixed well and centrifuged at 10,000*g* for 5 min at 4°C. The supernatant was transferred into a new RNase-free microfuge tube followed by RNA purification using the RNeasy® mini kit (Qiagen GmbH, Hilden, Germany), including an on-column DNase I (Roche Diagnostics GmbH, Mannheim, Germany) treatment according to the manufacturer's instructions. Quality of total RNA was verified and quantified using a NanoDrop ND-1000 spectrophotometer and Experion™ RNA StdSens Analysis Kit (Bio-Rad, Hercules, CA).

Five microgram of total RNA was first reverse-transcribed to cDNA, labelled, and purified using a FairPlay® Microarray Labeling Kit according to the one-colour microarray-based prokaryote analysis FairPlay® III labelling protocol (Agilent Technologies, ver.1.3). The quality and quantity of cDNA was confirmed using a NanoDrop ND-1000 spectrophotometer. About 600 ng of purified dye-coupled cDNA was hybridized onto a dual *D. hafniense* microarray targeting the genomes of *D. hafniense* strains DCB-2 and Y51 (see below for details) for 16 h at 65°C in a rotating Agilent hybridization oven, washed according to the FairPlay® III labelling protocol (Agilent Technologies, ver. 1.3) and scanned immediately on the Agilent DNA Microarray Scanner (G2505C) by using the one colour scan setting for 8 × 60 K array slides. Signal intensities were inferred from the obtained digital images using the Feature Extraction software (Agilent Technologies, Ver.10.7.3.1). Samples were hybridized to random positions of the 8-array containing slides. cDNA from an ammonium-deprived A2 chemostat was hybridized twice in order to provide a technical replicate for confirming technical reproducibility.

The microarray used in this study was custom-designed based on the complete genome sequences of *D. hafniense* DCB-2 and Y51 (NCBI Genbank accession numbers NC_007907 and NC_011830 respectively). The array contains 21905 distinct 45–60 oligonucleotides designed with

PICKY (Chou *et al*., 2004, 2009), including two or three probes per target transcript, as well as sense and antisense probes targeting intergenic regions larger than 60 oligonucleotides. Overall, the probe set was designed for 99% of all protein coding sequences and for 70% of intergenic regions for both strains. It included 2044 probes specific to 848 unique *D. hafniense* DCB-2 genes, 2803 probes specific to 1106 unique *D. hafniense* Y51 genes, 1927 probes specific to 1168 unique *D. hafniense* DCB-2 intergenic regions, 3479 probes specific to 1774 unique *D. hafniense* Y51 intergenic regions and 11,652 probes targeting genes and intergenic regions shared by both genomes. Probes were printed in duplicate on the Agilent 8 × 60 K custom gene expression microarray platform, containing in addition 1319 Agilent control probes.

ICPL, LC–MS/MS and proteome analysis

For proteomic analysis, 100 ml of liquid culture from batches and chemostats were taken and cells were harvested by centrifugation at 3300*g* for 20 min at 4°C and washed once with 1× phosphate buffered saline (PBS), containing per litre 8 g NaCl, 0.2 g KCl, 0.24 g KH_2PO_4 and 1.4 g Na_2HPO_4. The washed cell pellet was stored at –80°C until further analysis.

Protein extraction and stable isotope labelling used the ICPL Quadruplex kit (Serva, Heidelberg, Germany) according to the manufacturer's instructions. After thawing at room temperature, the cell pellet was dissolved in 400 µl of lysis buffer (guanidine hydrochloride) followed by ultra-sonication, twice for 1 min (0.3 s per pulse, 30% duty) (ultrasonic processor UP50H, Hielscher Ultrasonics, Germany) with sample cooling on ice between the rounds. Protein concentration was determined using the Bradford protein assay (Bio-Rad, Munich, Germany) (Bradford, 1976). Samples used for stable isotope labelling contained equal amounts of proteins (~5 mg ml^{-1}).

Stable isotope labelling of the extracted proteins was done with the ICPL Quadruplex kit (Serva) according to manufacturer's protocol. Four different ICPL labels (ICPL-0, ICPL-4, ICPL-6, ICPL-10) were used, one per growth condition (lactate-, fumarate-limitation, ammonium-deprivation and two different batch samples were used as references) (Supporting Information Table S1). Three analysis runs were performed. In order to analyse technical variability, chemostats F2 (fumarate-limited) and an A1 (ammonium-deprived; Note: ammonium-deprived chemostats were discarded for this manuscript) chemostat run in parallel, as well as batch experiment B2 were labelled and measured twice (Supporting Information Table S1). For each analysis, the isotope-labelled proteins from the four different treatments were combined. Labelled proteins were precipitated with acetone and separated by one-dimensional gel electrophoresis. After Coomassie Blue staining, each lane was cut into 5 or 6 slices and subjected to in-gel digestion with trypsin (Sigma Aldrich, Germany) as described previously (Merl *et al*., 2012). Digested peptides were separated by nano-HPLC and analysed with a LTQ Orbitrap XL mass spectrometer (Thermo Scientific, Germany; Gaupels *et al*., 2012). Up to 10, most intense, peptide-ion peaks were selected for fragmentation in the linear ion trap. Furthermore, peptides already selected for fragment analysis were dynamically excluded for 60 s. The cellular distribution of ICPL-labelled proteins corresponded to the distribution of all predicted proteins, suggesting that extraction and labelling of proteins was nonselective (Supporting Information Fig. S2).

Microarray and proteomic data analysis

All transcriptomic and proteomic data are presented as log 2 transformations of transcript intensity and protein signal intensity at a given limiting condition, taken relative to batch as a reference condition, and calculated as ratios. In this study, the BIOCONDUCTOR version 2.9 (http://www.bioconductor.org) based on the R programming language was used. R analysis packages such as limma, arrayQualityMetrics, marray and Agi4x44PreProcess were included to demonstrate the workflow of microarray data analysis for different *D. hafniense* genes annotation, normalization. The false discovery rate (FDR) was controlled below 1%. Differential gene expression was considered to be significant if the ratio of the hybridization signal intensities was two-fold or greater between two conditions (Johnson *et al*., 2008).

High array-to-array reproducibility was obtained for the parallel ammonium-deprived chemostat A2 technical replicates and between biological replicates of the batch experiments, with an R^2 (i.e., the coefficient of determination taken as the square of the Pearson correlation coefficient) of 0.96 and 0.97 respectively. Reproducibility among chemostat runs under approximately the same limiting conditions was relatively low ($R^2 < 0.8$). At the transcriptome level, ^{2}log(ratio)'s < –1 and > 1 showed fair reproducibility (75%–92% similarity if expressed in terms of correlation coefficient) between chemostats of the same limiting condition (Supporting Information Fig. S1B).

The microarray data have been submitted and accepted by Gene Expression Omnibus (GEO). The GEO accession number is GSE107146 which has been published online since November 22nd, 2017. (https://www.ncbi.nlm.nih.gov/geo/query/acc.cgi?acc=GSE107146)

For the proteome, the MS/MS spectra were searched against the *D. hafniense* database (downloaded from Uniprot and having 5017 sequences) using the Mascot search engine (version 2.3.02; Matrix Science) using a precursor mass error tolerance of 10 ppm and a fragment tolerance of 0.6 D. One missed cleavage was allowed. Carbamidomethylation was set as a fixed modification.

Oxidized methionine and ICPL-0, ICPL-4, ICPL-6 and ICPL-10 modifications for lysine residues were set as variable modifications. Data processing for the identification and quantification of ICPL-quadruplex labelled proteins was performed using Proteome Discoverer version 1.3.0.339 (Thermo Scientific, Germany). Proteome Discoverer automatically generated the ratios of signal intensities of peptide pairs labelled with different stable isotope labels. All possible ratios were generated for a given peptide within each labelling campaign. The Mascot Percolator algorithm was used for the discrimination between correct and incorrect spectrum identifications (Brosch *et al*., 2009), with a maximum q value of 0.01. Subsequently, protein ratios were calculated based on the median of all peptide ratios, which were identified to belong to a corresponding protein (Cox and Mann, 2008). Proteins were further filtered using the following two criteria: high peptide confidence (false discovery rate below 1%) and at least 2 peptides per protein (count only rank 1 peptide and count peptide only in top scored proteins).

Protein ratios of each measurement were normalized by the median of all protein ratios detected in Proteome Discoverer. Statistical analysis was performed separately for normalized ratios of each replicate using the Perseus statistical tool. Log 2 transformed protein ratios [^{2}log(ratio)'s] were used to quantify the probability of obtaining ratios significantly different from consistency with the main distribution (determined by Proteome Discoverer; Cox and Mann, 2008). This significance [termed Significance B according to (Cox and Mann, 2008)] was calculated for each protein group, which was created based on intensity bins. Each bin contained an equal number of proteins. Significance B was corrected for multiple testing by the false discovery rate (FDR) with significance cut off $p < 0.05$. Comparison between the number of proteins detected with LC–MS/MS analysis and the number of protein ratios generated by Proteome Discoverer, revealed that 82% of detected proteins were isotope-code labelled. Analysis of variability between technical replicates analysed in one run (fumarate-limited chemostat F2) and in two different runs (ammonium-deprived chemostat A1; Note: ammonium-deprived chemostats were discarded for this manuscript) did not reveal any run effect on the observed variation between generated protein ^{2}log(ratio)'s (Supporting Information Fig. S1A).

A lower reproducibility was achieved at the proteome level for all ^{2}log(ratio)'s in fumarate-, and lactate-limited chemostats (75%–89%, and 62% respectively) (Supporting Information Fig. S1C).

Acknowledgements

This work is dedicated to the memory of Dr Wilfred Röling, who passed away during preparation of this manuscript and who has been pivotal to its design.

We would like to thank Lauren Bradford for correcting the English of this manuscript. We thank Maria Suarez Diez for the help with bioinformatic analysis, especially with regards to the transcriptome analysis, Drs Fred Boogerd and Thomas Kruse for valuable comments on the final stage manuscript. We thank Prof. Dr. Masatoshi Goto, Department of Bioscience and Biotechnology, Faculty of Agriculture, Kyushu University, Japan for providing us with *D. hafniense* strain Y51.

This work was supported through various grants, including Synpol: EU-FP7 (KBBE.2012.3.4-02 #311815), BACSIN: EU-FP7 (KBBE-211684), Corbel: EU-H2020 (NFRADEV-4-2014-2015 #654248), and Epipredict: EU-H2020 MSCA-ITN-2014-ETN: Marie Skłodowska-Curie Innovative Training Networks (ITN-ETN) #642691, BBSRC China: BB/J020060/1.

References

Bansal, R., Helmus, R. A., Stanley, B. A., Zhu, J., Liermann, L. J., Brantley, S. L., and Tien, M. (2013) Survival during long-term starvation: global proteomics analysis of *Geobacter sulfurreducens* under prolonged electron-acceptor limitation *J Proteome Res*. **12**: 4316–4326.

Becker, J. G. (2006) A modeling study and implications of competition between *Dehalococcoides ethenogenes* and other tetrachloroethene-respiring bacteria *Environ Sci Technol*. **40**: 4473–4480.

Bradford, M. M. (1976) A rapid and sensitive method for the quantitation of microgram quantities of protein utilizing the principle of protein-dye binding *Anal Biochem*. **72**: 248–254.

Bradley, P. M., and Chapelle, F. H. (2010)Biodegradation of chlorinated ethenes . In *In Situ Remediation of Chlorinated Solvent Plumes*, Stroo, H. F., and Ward, C. H. (eds). New York, NY: Springer, pp. 39–67.

Brosch, M., Yu, L., Hubbard, T., and Choudhary, J. (2009) Accurate and sensitive peptide identification with mascot percolator *J Proteome Res*. **8**: 3176–3181.

Chou, H. H., Hsia, A. P., Mooney, D. L., and Schnable, P. S. (2004) PICKY: oligo microarray design for large genomes *Bioinformatics*. **20**: 2893–2902.

Chou, H. H., Trisiriroj, A., Park, S., Hsing, Y. I. C., Ronald, P. C., and Schnable, P. S. (2009) Direct calibration of PICKY-designed microarrays *BMC Bioinform*. **10**: 347.

Christiansen, N., and Ahring, B. K. (1996) *Desulfitobacterium hafniense* sp. nov., an anaerobic, reductively dechlorinating bacterium *Int J Syst Evol Microbiol*. **46**: 442–448.

Conrad, R., Schink, B., and Phelps, T. J. (1986) Thermodynamics of H2-consuming and H2-producing metabolic reactions in diverse methanogenic environments under *in situ* conditions *FEMS Microbiol Ecol*. **2**: 353–360.

Cox, J., and Mann, M. (2008) MaxQuant enables high peptide identification rates, individualized p.p.b.-range mass accuracies and proteome-wide protein quantification *Nat Biotechnol*. **26**: 1367–1372.

Direito, S. O. L., Ehrenfreund, P., Marees, A., Staats, M., Foing, B., and Roling, W. F. M. (2011) A wide variety of putative extremophiles and large beta-diversity at the Mars Desert Research Station (Utah) *Int J Astrobiol*. **10**: 191–207.

Esteve-Núñez, A., Rothermich, M., Sharma, M., and Lovley, D. (2005) Growth of *Geobacter sulfurreducens* under nutrient-limiting conditions in continuous culture *Environ Microbiol*. **7**: 641–648.

Franchini, A. G., and Egli, T. (2006) Global gene expression in *Escherichia coli* K-12 during short-term and long-term adaptation to glucose-limited continuous culture conditions *Microbiology*. **152**: 2111–2127.

Furukawa, K., Suyama, A., Tsuboi, Y., Futagami, T., and Goto, M. (2005) Biochemical and molecular characterization of a tetrachloroethene dechlorinating *Desulfitobacterium* sp strain Y51: a review *J Ind Microbiol Biotechnol*. **32**: 534–541.

Gaupels, F., Sarioglu, H., Beckmann, M., Hause, B., Spannagl, M., Draper, J., *et al*. (2012) Deciphering systemic wound responses of the pumpkin extrafascicular phloem by metabolomics and stable isotope-coded protein labeling *Plant Physiol*. **160**: 2285–2299.

Gottschalk, G. (1986) *Bacterial Metabolism*. New York, NY: Springer.

Hoskisson, P. A., and Hobbs, G. (2005) Continuous culture - making a comeback? *Microbiology*. **151**: 3153–3159.

Johnson, D. R., Brodie, E. L., Hubbard, A. E., Andersen, G. L., Zinder, S. H., and Alvarez-Cohen, L. (2008) Temporal transcriptomic microarray analysis of "*Dehalococcoides ethenogenes*" strain 195 during the transition into stationary phase *Appl Environ Microbiol*. **74**: 2864–2872.

Kim, S.-H., Harzman, C., Davis, J. K., Hutcheson, R., Broderick, J. B., Marsh, T. L., and Tiedje, J. M. (2012) Genome sequence of *Desulfitobacterium hafniense* DCB-2, a gram-positive anaerobe capable of dehalogenation and metal reduction *BMC Microbiol*. **12**: 21.

Kovarova-Kovar, K., and Egli, T. (1998) Growth kinetics of suspended microbial cells: from single-substrate-controlled growth to mixed-substrate kinetics *Microbiol Mol Biol Rev*. **62**: 646–666.

Kroger, A. (1974) Electron-transport phosphorylation coupled to fumarate reduction in anaerobically grown *Proteus rettgeri Biochim Biophys Acta*. **347**: 273–289.

Kruse, T., Goris, T., Maillard, J., Woyke, T., Lechner, U., de Vos, W., and Smidt, H. (2017) Comparative genomics of the genus Desulfitobacterium . *FEMS Microbiol Ecol*. **93**: fix135.

Kruse, T., van de Pas, B. A., Atteia, A., Krab, K., Hagen, W. R., Goodwin, L., *et al*. (2015) Genomic, proteomic, and biochemical analysis of the organohalide respiratory pathway in *Desulfitobacterium dehalogenans J Bacteriol*. **197**: 893–904.

Marozava, S., Röling, W. F. M., Seifert, J., Köffner, R., von Bergen, M., and Meckenstock, R. U. (2014) Physiology of *Geobacter metallireducens* under excess and limitation of electron donors. Part II. Mimicking environmental conditions during cultivation in retentostats *Syst Appl Microbiol*. **37**: 287–295.

Meckenstock, R. U., Elsner, M., Griebler, C., Lueders, T., Stumpp, C., Aamand, J., *et al*. (2015) Biodegradation: updating the concepts of control for microbial cleanup in contaminated aquifers *Environ Sci Technol*. **49**: 7073–7081.

Merl, J., Ueffing, M., Hauck, S. M., and von Toerne, C. (2012) Direct comparison of MS-based label-free and SILAC quantitative proteome profiling strategies in primary retinal Mueller cells *Proteomics*. **12**: 1902–1911.

Mingo, F. S., Studenik, S., and Diekert, G. (2014) Conversion of phenyl methyl ethers by *Desulfitobacterium* spp. and screening for the genes involved *FEMS Microbiol Ecol*. **90**: 783–790.

Nonaka, H., Keresztes, G., Shinoda, Y., Ikenaga, Y., Abe, M., Naito, K., *et al*. (2006) Complete genome sequence of the dehalorespiring bacterium *Desulfitobacterium hafniense* Y51 and comparison with *Dehalococcoides ethenogenes* 195 *J Bacteriol*. **188**: 2262–2274.

Overkamp, W., Ercan, O., Herber, M., Maris, A. J., Kleerebezem, M., and Kuipers, O. P. (2015) Physiological and cell morphology adaptation of *Bacillus subtilis* at near-zero specific growth rates: a transcriptome analysis *Environ Microbiol*. **17**: 346–363.

Peng, X., Yamamoto, S., Vertes, A. A., Keresztes, G., Inatomi, K.-I., Inui, M., and Yukawa, H. (2012) Global transcriptome analysis of the tetrachloroethene-dechlorinating bacterium *Desulfitobacterium hafniense* Y51 in the presence of various electron donors and terminal electron acceptors *J Ind Microbiol Biot*. **39**: 255–268.

Plugge, C. M., Dijkema, C., and Stams, A. J. M. (1993) Acetyl-CoA cleavage pathway in a syntrophic propionate oxidizing bacterium growing on fumarate in the absence of methanogens *FEMS Microbiol Lett*. **110**: 71–76.

Plugge, C. M., Henstra, A. M., Worm, P., Swarts, D. C., Paulitsch-Fuchs, A. H., Scholten, J. C. M., *et al*. (2012) Complete genome sequence of *Syntrophobacter fumaroxidans* strain (MPOBT) *Stand Genom Sci*. **7**: 91–106.

Ragsdale, S. W., and Pierce, E. (2008) Acetogenesis and the wood-Ljungdahl pathway of CO_2 fixation *BBA-Prot Proteom*. **1784**: 1873–1898.

Rossell, S., van der Weijden, C. C., Kruckeberg, A. L., Bakker, B. M., and Westerhoff, H. V. (2005) Hierarchical and metabolic regulation of glucose influx in starved *Saccharomyces cerevisiae FEMS Yeast Res*. **5**: 611–619.

Rossell, S., van der Weijden, C. C., Lindenbergh, A., van Tuijl, A., Francke, C., Bakker, B. M., and Westerhoff, H. V. (2006) Unraveling the complexity of flux regulation: a new method demonstrated for nutrient starvation in *Saccharomyces cerevisiae Proc Natl Acad Sci U S A*. **103**: 2166–2171.

Rossell, S., Lindenbergh, A., Van Der Weijden, C. C., Kruckeberg, A. L., Van Eunen, K., Westerhoff, H. V., and Bakker, B. M. (2008) Mixed and diverse metabolic and gene-expression regulation of the glycolytic and fermentative pathways in response to a HXK2 deletion in *Saccharomyces cerevisiae FEMS Yeast Res*. **8**: 155–164.

Smidt, H., and de Vos, W. M. (2004) Anaerobic microbial dehalogenation *Annu Rev Microbiol*. **58**: 43–73.

Stouthamer, A. H., and Bettenhaussen, C. W. (1975) Determination of the efficiency of oxidative phosphorylation in continuous cultures of *Aerobacter aerogenes Arch Microbiol*. **102**: 187–192.

Suyama, A., Iwakiri, R., Kai, K., Tokunaga, T., Sera, N., and Furukawa, K. (2001) Isolation and characterization of *Desulfitobacterium* sp strain Y51 capable of efficient dehalogenation of tetrachloroethene and polychloroethanes *Biosci Biotech Biochem*. **65**: 1474–1481.

Ter Kuile, B. H., and Westerhoff, H. V. (2001) Transcriptome meets metabolome: hierarchical and metabolic regulation of the glycolytic pathway *FEBS Lett*. **500**: 169–171.

Thauer, R. K., Jungermann, K., and Decker, K. (1977) Energy conservation in chemotrophic anaerobic bacteria *Bacteriol Rev*. **41**: 100–180.

Trautwein, K., Lahme, S., Woehlbrand, L., Feenders, C., Mangelsdorf, K., Harder, J., *et al*. (2012) Physiological and proteomic adaptation of *"Aromatoleum aromaticum"* EbN1 to low growth rates in benzoate-limited, anoxic chemostats *J Bacteriol*. **194**: 2165–2180.

Van Verseveld, H. W., Chesbro, W. R., Braster, M., and Stouthamer, A. H. (1984) Eubacteria have 3 growth modes keyed to nutrient flow - consequences for the concept of maintenance and maximal growth-yield *Arch Microbiol*. **137**: 176–184.

Vignais, P. M., and Billoud, B. (2007) Occurrence, classification, and biological function of hydrogenases: an overview *Chem Rev*. **107**: 4206–4272.

Villemur, R., Lanthier, M., Beaudet, R., and Lepine, F. (2006) The *Desulfitobacterium* genus *FEMS Microbiol Rev*. **30**: 706–733.

Von Stockar, U., and Liu, J. S. (1999) Does microbial life always feed on negative entropy? Thermodynamic analysis of microbial growth *Biochim Biophys Acta*. **1412**: 191–211.

Westerhoff, H. V., and Van Dam, K. (1987) *Thermodynamics and Control of Biological Free-Energy Transduction*. Amsterdam: Elsevier Science Ltd.

Zaunmuller, T., Kelly, D. J., Glockner, F. O., and Unden, G. (2006) Succinate dehydrogenase functioning by a reverse redox loop mechanism and fumarate reductase in sulphate-reducing bacteria *Microbiology*. **152**: 2443–2453.

Zehnder, A. J. B. (1989) *Biology of Anaerobic Microorganisms*. New York, NY: John Wiley and Sons.

Zhang, T., Nevin, K., Barlett, M., Gannon, S., Bain, T. and Lovley, D.R. (2011) Anaerobic benzene degradation by *Geobacter* species with Fe(III) or an electrode as the electron acceptor. In *The 111th General Meeting of the American Society of Microbiology.* New Orleans, LA.

Zoetendal, E. G., Heilig, H., Klaassens, E. S., Booijink, C., Kleerebezem, M., Smidt, H., and de Vos, W. M. (2006) Isolation of DNA from bacterial samples of the human gastrointestinal tract *Nat Protoc*. **1**: 870–873.

Supporting Information

Additional Supporting Information may be found in the online version of this article at the publisher's web-site:

Appendix S1: SUPPORTING INFORMATION.

Table S1: Labelling strategy and arrangement of labelled proteins in labelling campaigns. **A***: ammonium deprivation, **F**: fumarate limitation, **L**: lactate limitation. In each analysis run ICPL-0 was used to label proteins extracted from batch.

Table S2: mRNAs and proteins detected in all biological replicates (excel table).

Table S3: Simulation of experimental data of Table 2 in terms of 4 processes described in Table 1 plus process related to biomass formation. Process 0: biomass synthesis; Process 1: reduction of fumarate by lactate; Process 2: fumarate disproportionation; Process 3: lactate fermentation to ethanol and carbon dioxide; and Process 4: lactate fermentation to acetate, carbon dioxide and hydrogen. Process intensities (fitted; in normal type) are given in mM as the metabolite concentrations. C-rec total: Carbon recovery (Equation 5; 100% would be perfect prediction). e-rec: electron recovery (Equation 6; 100% would be perfect prediction). Experimental input values are in italics.

Table S4: Excel file with calculation of delta G correction.